Alkali activated slag concretes designed for a desired slump, strength and chloride diffusivity

Bondar, D., Ma, Q., Soutsos, M., Basheer, M., Provis, J. L., & Nanukuttan, S. (2018). Alkali activated slag concretes designed for a desired slump, strength and chloride diffusivity. *Construction and Building Materials*, *190*, 191-199. https://doi.org/10.1016/j.conbuildmat.2018.09.124

Published in:
Construction and Building Materials

Document Version:
Peer reviewed version

Alkali activated slag concretes designed for a desired slump, strength and chloride diffusivity

Dali Bondar[1], Qianmin Ma[2], Marios Soutsos[1], Muhammed Basheer[3], John L. Provis[4], Sreejith Nanukuttan[1]

[1]School of Natural and Built Environment, Queen's University Belfast, BT9 5AG, UK

[2]Faculty of Civil Engineering and Mechanics, Kunming University of Science and Technology, 650500 Kunming, China

[3]School of Civil Engineering, University of Leeds, LS2 9JT, UK

[4]Department of Materials Science and Engineering, University of Sheffield, S1 3JD, UK

Email: d.bondar@qub.ac.uk, maqianmin666@163.com, m.soutsos@qub.ac.uk, P.A.M.Basheer@leeds.ac.uk, J.Provis@Sheffield.ac.uk, s.nanukuttan@qub.ac.uk

Abstract

Ground granulated blast furnace slag (GGBS) is the most common industrial by-product used as a precursor for alkali activated binders due to its fast setting, simple curing needs, and good early age strength gain. There are conflicting findings on the chloride penetration resistance of such binders and more information is required regarding the suitability of this type of binder material for chloride environments. This article outlines the findings of investigation of alkali activated slag concretes (AASC), to provide a comprehensive view of the effect of mix design variables on slump, strength, and chloride transport and binding. It is concluded that AASC can be designed for different workability and different grades of concrete. The diffusivity results demonstrate that the addition of excess water does not directly control the pore structure/connectivity in AASC as it does for Portland cement, and therefore AASC can be designed based on the water/binder ratio needed for a specified mechanical performance. The chloride binding capacity increased as the paste content of the concrete and/or the silica content of the activator was increased.

Keywords: alkali activated slag concretes (AASC); workability; strength; chloride diffusion and chloride binding capacity

1. Introduction

Alkali activated materials (AAMs) have been under consideration as an alternative binder system since 1895 [1]. However, despite the engineering community having been aware of the potential of this material for over a century, there is still insufficient information available about the durability of AAMs, and the resistance to chloride ingress is particularly critical for materials intended to serve in reinforced concretes.

Several factors are known to affect the setting time, workability, strength and durability properties of alkali activated slag concretes (AASC), including: the type of alkaline activator, the means of adding the activator, the dosage of alkali, the SiO_2/Na_2O ratio (denoted *modulus*, Ms), the type and fineness of slag, the paste content of the concrete, and the water to solid ratio in the paste constituent of AASC.

Many of these factors are interdependent, and the effect of changing more than one in parallel is usually not additive. The optimum Na_2O dosage for AAS binders activated by sodium silicate solution under normal curing has been found to be 3% – 5% relative to the mass of slag, depending on the demand for high early age strength [2-4]. Slag cements activated by sodium silicate at modulus values between 0.6 and 1.5 at appropriate dosages were reported to show high ultimate strength for engineering purposes. However, this optimum modulus for appropriate dosage of sodium silicate varied depending on the type of slag, i.e. 0.75 – 1.25 for acid slag, 0.90 – 1.3 for neutral slag, and 1.0 – 1.5 for basic slag [3-5]. Activation by sodium silicate tends to give higher strength than when NaOH is used; the lower strength in the NaOH activated slag pastes may be explained by the much higher porosity found in these pastes than in the sodium silicate activated materials [6].

The effect of water to slag ratio on NaOH activated slag is similar to that of water to cement ratio on Portland cement [4]. However, an increase in water to slag ratio has a very marked effect to decrease the heat evolution of Na_2SiO_3 activated slag [4]. In this case when the water to solid/slag ratio is lower than 0.45, there is an early and pronounced peak in the heat evolution curve, which then changes to a very diffuse peak with 15 hours delay for a water to slag ratio greater than 0.45 [4]. This can have a noticeable effect on the performance of AASC, especially on workability and setting time.

It has been reported [7] that by controlling mix design parameters, such as binder content and water to binder ratio, it is possible to produce AASC with mechanical strength and durability comparable to conventional Portland cement concretes. It has also been shown that a higher slag content leads to an increase in strength of AASC and improvement of the permeability, water absorption and carbonation resistance [7].

Park *et al.* [8], in their work using mortars, have reported that the corrosion behaviour of embedded steel in AAMs was strongly dependent on the type of alkali activator. According to their findings, AAS containing $Ca(OH)_2$ as the activator was most effective to reduce galvanic corrosion, while KOH and NaOH activators indicated corrosion levels similar to that of Portland cement mortar [8].

AASC has traditionally been known for its low slump, and this raises challenges in its design for different workabilities and different grades of concrete. Therefore, this article presents findings from investigations of the effect of water/slag ratio and binder content on workability, strength, chloride diffusion and chloride binding in AASC, with the aim of determining the suitability of AASC for use in chloride environments. The outcomes will help designers to select mix designs for AASC for required performance.

2. Materials and experimental procedures

2.1 Materials

The granulated blast furnace slag used in this study was provided by ECOCEM, France. The basicity coefficient ($CaO+MgO/SiO_2+Al_2O_3$) and the quality coefficient ($(CaO+MgO+Al_2O_3)/(SiO_2+TiO_2)$) were calculated from the chemical composition (Table 1) to be 1.07 and 1.7, respectively. The particle size distribution of slag was determined by laser diffraction, the particle density was measured using a LeChatelier flask, and the water absorption was measured using the centrifugal consolidation method; these physical properties are presented in Table 2.

The aggregates used in this study were crushed basalt from local sources in Northern Ireland, and comprised 10 mm and 16.5 mm crushed aggregates, and 4 mm sand. In stage A of the experimental campaign, the proportion of 16.5:10:4 mm fractions were 32:32:36; in stage B the proportions were optimised for the best packing density at 48:12:40. The bulk specific gravity and water absorption of these materials were measured based on BS EN 1097-1, and are presented in Table 3. Potable tap water (i.e. drinking water quality) was used to make the concrete mixes.

Sodium hydroxide (NaOH) pellets were dissolved in water and used along with sodium silicate solution to act as alkaline activators in concrete production at specified concentrations and compositions, as shown in Table 4. The chemical composition of the as-received sodium silicate solution was 15.5% sodium oxide (Na_2O), 30.5% silicon dioxide (SiO_2) and 54% water, on a mass basis. NaOH was used to adjust the Na_2O content and Ms value to the required values.

2.2 Mix details, mixing and casting of test specimens

Twelve AAS concretes with alkali concentrations (Na_2O % by of mass of slag) of 4, 6, and 8 %, and modulus (Ms) values of the sodium silicate solution activator of 0.75, 1.00, 1.50, and 2.00, were studied in stage A. The water/binder mass ratio (w/b) was held constant at 0.47 in these concretes. A barium based retarder was used in this work for mixes A1-A12 for controlling the setting time. The content of the retarder was 0.3% of the mass of slag for all of these mixes and dry-blended with slag before mixing. For the purpose of comparison, one PC concrete mix was manufactured with the same total binder content as that of the AAS concretes. A w/b of 0.42 was specified for the PC concrete [9] to ensure that its performance in exposure classes XS3 and XD3 as defined in BS EN 206:2013 [10] would be acceptable. In stage B, ten further AAS concretes were studied with different w/b ratios, binder to aggregate ratios, alkali concentrations, and Ms values without using retarder. The details of the different mixes and their initial properties are presented in Table 4. Throughout this work, the total binder content is defined as the sum of GGBS and the solid component of the sodium silicate solution, and the water content of the sodium silicate solution was taken into account while determining the mixing water.

A laboratory pan-mixer of volume 50 L was used in this study. In stage A the mixing was conducted in accordance with BS 1881-125:2013 [11]. In Stage B, crushed basalt aggregates and sand were first dry-mixed together for one minute, and the GGBS powder was subsequently added, and mixed for a further 2 minutes. The sodium hydroxide solution was then added and after a further 2 minutes of mixing, then sodium silicate solution was added and mixing continued for a further minute.

For both stages, fresh properties of concrete were measured according to BS EN 12350 [12], and nine 100 mm cubes and one 250×250×110 mm slab were cast for determining compressive strength in accordance with BS EN 12390 [13], and chloride diffusion coefficients according to Nordtest NT Build 443 [14]. After casting, all the specimens (still in moulds) were covered with plastic sheets and left in the casting room for 24 h. The demoulded slabs were wrapped with 3 layers of plastic sheets, and cube samples were kept in a sealed plastic zip bag, until the testing date. The storage room was maintained at 23ºC and 65% RH.

2.3 Testing procedures

Chloride transport through AAS concretes was assessed using a non-steady state chloride diffusion test, Nordtest NT Build 443 [14]. One day before the test age of 91 days, three cores of diameter 100 mm per mix were drilled from the 250 x 250 x 110 mm concrete blocks. A slice with a thickness of 50 mm from the cast surface (trowel finished face) was cut off, and the rest was kept for carrying out the test. The vacuum saturation regime specified in the standard was used to precondition the slices so that the chloride flow is predominantly diffusive, and initial sorption or capillary forces are negligible. The vacuum was applied to remove air for three hours and released afterwards. Samples were wrapped in hessian saturated in deionised water to prevent leaching of ions, and placed in the container. The weight of the sample was noted after an hour (W_1) and then vacuum was applied, followed by further saturation. Weight was checked again (W_2). Usually after 6 hours, when W_i-$W_{(i-1)}$ was less than 0.1%, the samples were considered fully saturated; if not, saturation was continued until this criterion was met. After conditioning to a surface-dry condition, an epoxy resin was applied onto the surfaces of the specimens in three layers except the exposure face (saw cut face). When the epoxy coating was dry, the cores were immersed in an NaCl solution of concentration 165 g/L (~2.82 M) for three months for samples tested in stage A, or six months for samples tested in stage B. After immersion, the cores were profile ground to obtain concrete dust from different depths up to a depth of 30 mm in stage A and 16 mm in stage B, measured from the exposed surface. The total chloride content of the dust samples was determined in accordance with the recommendations of RILEM TC 178-TMC [15] using a pre-calibrated potentiometric titration method. The concrete dust was dissolved in deionised water in accordance with RILEM TC 178-TMC recommendations [16] to measure the pH value of the suspension in both stages, and for the determination of water soluble chlorides in stage B. Chloride diffusivity and the surface

chloride content were determined by using curve fitting to the error function solution of Fick's second law of diffusion, as described in NT BUILD 443 [14].

3. Results and discussion

The following sections discuss the slump, compressive strength, chloride diffusivity, and chloride binding capacity of AAS concretes.

3.1 Slump

AASC has often been characterised by a low slump value and rapid setting behaviour; slump values up to 60-120 mm have been reported in the literature [17]. The purpose of this testing programme was to demonstrate the range of slump values that AASC is capable of producing, and the changes to the governing variables that are necessary to achieve such high slump. The Stage A results shown in Table 4 and Figure 1 indicate that a slump value between 55-180 mm can be achieved by varying the percentage Na_2O and Ms while the w/b is fixed at 0.47. As the percentage of Na_2O increased, the slump increased from 55-70 mm (Mixes A1, A5 and A9), and a further increase in modulus (A1-A4, A5-A8, A9-12) brought the slump values to 180 mm due to the plasticising effects of dissolved silicate anions. In order to design slump class ≥ S3 specified in BS 8500-1:2015 [18], an Na_2O dose of 8% is required. The role of parameters such as Na_2O% and Ms in controlling the slump has been widely reported in the literature [19, 20] and is in agreement with the Stage A results.

In Stage B, tests were designed to consider the effects of other parameters such as w/b and binder content and did not use the retarder. Mixes in this stage were limited to Ms values of 0.45 or 1, as an increase in modulus means a proportional increase in the sodium silicate content, which is both costly and can have high negative environmental impacts. The main difference between the mix designs in the two stages is that w/b was increased to 0.55 in stage B, and its effect is very obvious on the slump as mixes B4, B6-B10 had slump values in excess of 135 mm. What is more interesting is that slump values >200 mm are achievable with low Na_2O% and Ms by increasing w/b, so in this sense, the AASC behaves similarly to PC concretes without any observation of bleeding or segregation.

As is evident from Figure 1a and 1b, the AASC can be designed for all slump ranges. However, higher slumps in the range of S4-S5 require w/b ratios higher that those allowed in BS 8500 [18]. Whether such high w/b ratios are acceptable for concretes in different chloride exposure environments will be further discussed in section 3.3, after the diffusivity results are presented.

The contour map graphs in Figure 2 show the results obtained for slump as a function of sodium oxide (Na_2O%) and silicate modulus (Ms), for different mixes with same binder content for both stages. Using a w/b ratio of 0.55 instead of 0.47 resulted in more workable mixes. It is obvious from Figure 2(b) that at higher w/b, both sodium oxide (Na_2O%) & silica modulus (Ms) have a significant effect on workability, while for lower w/b, parallel lines in Figure 2 (a) indicates that only the effect of Na_2O%

is significant. All AAS concrete mixes in stage 2 (i.e., 0.55 w/b) are in at least class S3 specified in BS 8500-1:2015 [18], even for the minimum alkali content and silica modulus, which are 4% and 0.45, respectively in this stage, whereas in stage A the minimum alkali content to reach this class of workability was more than 7.5% and the minimum silica modulus is 1.0. It is evident from the results in stage B that for a silica modulus more than 0.8, increasing the sodium oxide increases the workability, as has been reported by previous investigators [18, 19].

3.2 Compressive strength

An overall comparison of the results between Stages A and B (Figure 3) makes the effect of w/b very apparent, with almost all (except one) Stage A mixes exceeding 45 MPa at 28 days. Stage B mixes with w/b between 0.55 and 0.7 offer 28-day compressive strengths in the range 21.5 to 64.4 MPa. From the Stage A results, it can also be stated that: (1) most mixes had approximately 20 MPa after 3 days curing, (2) higher modulus results in loss of early strength, but offers comparable strength in the long term, (3) in most cases 28 day strength is 80-90% of the 91 day strength, offering insight into the short and long term microstructural development in such binders. It is obvious that mixes with high modulus (i.e., silicate content) need to be cured longer. Concretes with Ms values of 1.0 to 1.5 generally obtained the highest compressive strength (see Figure 3(a)), which is in agreement with the literature [21].

Figure 3b shows data for mixes with varying w/b. The comparable mixes B8-10 all offer better strengths than their Stage A equivalents (A2, A6, A10) after 28 days, despite their higher w/b. But as time progress, i.e., with 91 days curing, the aforementioned differences become negligible. Better strengths for Stage B could be due to their higher density. Due to these differences, it is best to summarise that strength in the range of 20-60 MPa is achievable by altering the binder content, w/b, Ms, and Na_2O%. To aid with the design for strength, a contour map using 28 day compressive strength results as a function of sodium oxide (Na_2O%) and silica modulus (Ms) is provided in Figure 4. An increase of Na_2O% and Ms generally increases the compressive strength, which is in agreement with the results reported by others [19, 21]. This is due to the higher degree of reaction (indicating the extent to which the slag particles are reacted) caused by an increase in the alkali activator dosage [22]. More N-A-S-H (sodium alminosilicate hydrate) gels are generated when the Na_2O% and SiO_2 content are increased. The bottom right corner of Figure 4a (Stage A results) also shows that the strength value decreases as the silica modulus increases beyond 1.5 for Na_2O doses below 5%, as the alkalinity of the activators in such systems is not sufficient to reach a very high degree of reaction.

The PC concrete in Stage A was designed as a reference that conforms to the BS EN 206:2013 requirement for exposure classes XS3 and XD3. Therefore, it was designed for a minimum characteristic compressive strength of 45 MPa, which is equivalent to an average strength ≥ 49.41 MPa (calculated as 45 +1.48(3.15) MPa; where 3.15 is the standard deviation of the test results). Table 4 and Figure 3(a) both show that mixes no. A3(4%-1.5), A6(6%-1.0), A7(6%-1.5), A8(6%-2), A9 (8%-0.75),

A10 (8%-1.0), A11(8%-1.5), A12(8%-2) and the PC met the strength requirements for this exposure class. Additionally, most of the AAS concretes except mix A4(4%-2) met the strength requirement of 41.66 (=37+1.48(3.15)) MPa for the lower-demand exposure classes XS1, XD1 and XD2. It should be noted that the w/b ratio used for AAS concretes (0.47) was higher than that for PC concrete (0.42) due to the lack of workability of the AAS at such a low water content [9]. The 28 day compressive strength results reported for stage B in Table 4 and Figure 3(b) show that mixes B7(8%-0.45), B9(6%-1) and B10(8%-1) also achieved the required strength ≥ 51.11 (=45+1.48(4.13)) MPa for the exposure classes XS3 and XD3 even at w/b = 0.55. However, for mix B10 the setting time was inconveniently short, at around half an hour. Mixes B6(6%-0.45) and B8(4%-1) seem to meet the strength requirements of 43.11 (=37+1.48(4.13)) MPa for the exposure classes XS1, XD1 and XD2. Although it was evident that the strength requirement and w/b ratio of mixes B1, B2, B3 and B5 will not comply with BS EN 206:2013 norms, the intention of including these mixes was to assess their performance against chloride ingress and compare that data against a conforming PC reference.

Figure 5 shows the 91-day compressive strength results as a function of the SiO_2 content of the activator, relative to the total slag content (calculated for each mix as $Na_2O\% \times Ms$). When the 91-day compressive strength values of all the activated slag concrete mixes studied are plotted as a function of ($Na_2O\% \times Ms$), a two-term exponential relationship can be fitted, as shown in Fig. 5. In general, there is an increase in the 91-days compressive strength values with increase in the SiO_2 content, up to a value of ~ 9% of the total slag content. This parameter is significant because it has been shown that the later-age compressive strengths of activated slag concretes are proportional to the SiO_2 content of the activator [23], and a higher silicate content in the activator has been reported to lead to a higher degree of reaction [24]. In agreement with this observation, the results here support the use of the maximum SiO_2 content for optimising strength.

3.3 Chloride diffusivity through AASC

Figure 6 presents chloride diffusion coefficients, D_{nssd}, for mixes from both stages. Stage A mixes, at w/b = 0.47, show very low to low chloride diffusivity values as identified in the classification of RILEM TC 230-PSC [24], from 1.88×10^{-12} m^2/s [A7 (8%-1.5)] to 6.59×10^{-12} m^2/s [A1 (4%-0.75)]. Stage B mixes, with w/b values of 0.55-0.7, demonstrate low to very low chloride diffusivity values [25], from 5.09×10^{-12} m^2/s (B4) to 1.18×10^{-12} m^2/s (B2). All of the coefficients obtained, with the exception of A1, were lower than 6×10^{-12} m^2/s, which is the lowest limiting value specified for the equivalent durability approach in PD CEN/TR 16563 [26] for chloride environments. The coefficients obtained in this study are also similar to the non-steady state chloride migration coefficient values measured via NT Build 492 and reported elsewhere [27-29]. Comparing the results of the two stages illustrates that despite the high w/b ratio, stage B concretes offer lower diffusion coefficients. This could be due to better workability and compaction in the case of stage B mixes. All the D_{nssd} values for AAS concretes

were lower than the result shown for PC concrete in Figure 6(a), despite the higher water to binder ratio of the AASC mixes. This is possibly due to the influence of the activated aluminosilicates, chloride binding, pore size and pore connectivity of the concrete.

The effects of w/b and binder content are not directly obvious from the results. It seems that the excess water is not affecting the pore structure/connectivity of AASC as it does for PC concrete. Therefore, it can only be identified that mix design parameters and also reactivity of the aluminosilicate precursor [30] may have a larger influence on the diffusivity.

The contour plot in Figure 7(a) (stage A) indicates that for lower w/b an optimum can be achieved by increasing the Na_2O% and bringing the modulus closer to 1.5. The information in Figure 7(b) for stage B gives a lower range: (i) for Na_2O doses less than 5%, the lowest value is observed at a higher Ms, similar to the observations in Figure 7(a), and (ii) for higher Na_2O doses, this is reversed.

In summary, the D_{nssd} is comparatively low for all of the AASC mixes studied here. D_{nssd} is a measure of the rate of transport as modified by the chemical reactions leading to chloride binding. In order to distinguish these two effects, the binding capacity of the mixes in stage B was assessed to develop a more complete picture of the factors controlling chloride transport in AASC.

3.4 Chloride binding in AASC

There is limited information available on chloride binding of AASC in the literature. The available CSH and aluminate phases (C-(N)-A-S-H or two layered double hydroxides) in activated GGBS may contribute to the physical and chemical binding reactions [30, 31]. Figure 8 shows the total and water-soluble chloride concentrations measured for concrete mixes B8, B9 and B10, and the corresponding pH values are also provided for comparison. It is evident from Figure 8 that the surface region, Zone 1, is undergoing leaching-induced changes during Cl^- transport that result in a lowering of pH; there is also a skin effect which causes a near-surface dip in the total Cl^- content. The depth of zone 1 is between 5-12 mm for the three mixes; the lowest depth is for the mix with 6% Na_2O and Ms = 1. In Zone 2, pH reduction is not significant. It is known that pH reduction can release the Cl^- otherwise bound to Friedel's salt [32] in PC based systems. It should be noted that the total Cl^- is composed of both bound and free chloride, and free chloride is represented here by the water soluble fraction which therefore will also contain a proportion of the adhered Cl^- physically bound to the aluminate phases. The ratio between total and water-soluble Cl^- seems to follow the general trends established for PC systems [33]. The quantity of bound chlorides for all the mixes in stage B is shown in Table 5. This is computed by determining the area under the total and free chloride curves from the concentration vs depth graph (typical data shown in Fig. 8); the difference between the two areas gives the quantity of bound chloride. The values presented in Table 5 show that quantity of bound chlorides increased as the paste content of the concrete and/or the silica content of the activator was increased. As discussed, the main reaction product in AASC is an Na-Al substituted calcium silicate hydrate (C-(N)-A-S-H) gel which can bind

chlorides, while hydrotalcite-group minerals are a smaller constituent of the phase assemblage but have strong chloride binding capacity. Surface absorption is the main binding mechanism in these phases, responsible for around 90% of the total chloride uptake, with around 10% contribution from ion exchange [30, 31]. The binding capacity is comparable to the values reported for PC and high-volume blast furnace slag concrete [34]. This is likely due to the alkalinity reduction affecting the stability of the bound chlorides [34, 35] in zone 1.

In summary, the mass transport testing showed that AASC performed significantly better than conventional PC based binders in terms of restricting Cl^- transport. These concretes can be classified into two zones, based on the reduction of pH closer to the surface. While the overall binding capacity is deemed slightly lower than comparable PC systems, further study is needed to exclude the effect of pH reduction and to eliminate near-surface effects.

4. Conclusion

- AAS concretes can be designed for different workability and strength grades of concrete. The key parameters at the disposal of the designer are Na_2O%, Ms, and the paste content.
- For higher water to binder ratio, both sodium oxide (Na_2O%) and silica modulus (Ms) influence the workability, while for lower w/b only Na_2O% seems to have a notable effect.
- The compressive strength values were strongly proportional to the SiO_2 content in the activator. This will be useful as guidance to produce AASC of required strength.
- Chloride diffusion coefficients of AAS concretes are low. Measurement of chloride binding capacity was affected by the pH reduction due to leaching in the surface zone. The depth of the affected zone was in the range of 5-12 mm, so further study is required to discern the binding capacity of zones unaffected by this type of pH reduction.
- The diffusivity results demonstrate that the excess water is not affecting the pore structure/connectivity in AASC as it does for PC concretes; and AASC can be designed based on the w/b needed for a required mechanical performance.

As a closing remark the authors suggest adopting a performance-based approach to specifying such concretes, since the conventional wisdom of w/b and mix design features may not translate well [26]. A performance-based approach is apt to give confidence to the suppliers, and also to convince clients of the beneficial aspects of AASC.

309 Table 1: Oxide composition of the GGBS used, from X-ray fluorescence analysis

Precursor	Component (mass % as oxide)							
	SiO_2	Al_2O_3	CaO	Fe_2O_3	MgO	TiO_2	Other	LOI*
GGBS	35.7	11.2	43.9	0.3	6.5	0.512	1.578	0.31

310 * LOI is loss on ignition at 1000°C.

311 Table 2: Physical properties of the GGBS used

Fineness (particles ≥45μm)	7.74%
Particle density	2.86
Water absorption	35.14%

312

313 Table 3: Physical properties of aggregates

Aggregates	Bulk dry specific gravity	Bulk saturated surface-dry specific gravity	Water absorption (%)
Sand (0-4 mm)	2.72	2.73	0.75
Fine crushed agg. (5-10 mm)	2.67	2.75	3.14
Coarse crushed agg. (10-16 mm)	2.60	2.67	2.60

314

315 Table 4 (a): The details of the different Stage A mixtures and their properties

Mix No.	Mix details (Na_2O%-Ms)	Wet density	Setting time (initial/final) (min)	Slump (mm)	3 days compressive strength (MPa)	28 days compressive strength (MPa)	Concrete grade
A1	4%-0.75	2245	30/39	55	22.3	44.7	C32/40
A2	4%-1	2217	11/14	55	21.8	46.7	C35/45
A3	4%-1.5	2229	15/22	55	1.7	49.5	C35/45
A4	4%-2	2186	18/24	55	1.4	33.3	C30/37
A5	6%-0.75	2222	28/38	65	31.7	47.3	C35/45
A6	6%-1	2219	12/22	65	37.3	53.6	C40/50
A7	6%-1.5	2221	14/22	65	20.3	60.8	C49/60
A8	6%-2	2236	32/42	75	8	59.6	C45/55
A9	8%-0.75	2208	16/26	70	32.3	51.9	C40/50
A10	8%-1	2230	46/58	105	32.7	53.6	C40/50
A11	8%-1.5	2233	37/56	145	34.1	59.3	C45/55
A12	8%-2	2241	-	180	11.7	55.4	C45/55
A13	PC	2257	-	50	35.4	58.9	C45/55

316 Note: all have water to binder ratio = 0.47, binder content = 400 kg/m^3, sand = 670±16 kg/m^3 and aggregate = 1190±30
317 kg/m^3), from [9]. The setting time of the alkali activated slag pastes with standard consistence ($0.2<w/b<0.27$) was studied in
318 satge A and the results are reported in the above Table. Due to the quick setting as observed, a retarder described in section
319 2.2 at a dosage of 0.3% of the mass of slag was used to control the setting of the AASCs. This dosage was the minimum one
320 guaranteeing all of the alkali activated slag mixes to meet the setting time requirement specified in BS EN 197-1 (2011)
321 [36, 37].

322

Table 4 (b): The details of the different Stage B mixtures and their properties

Mix No.	Mix (Na_2O%-Ms)	Binder (kg/m^3)	w/b	Sand (kg/m^3)	Aggregate (kg/m^3)	Wet density	Setting time (initial/ final) (min)	Slump (mm)	2 days compressive strength (Mpa)	28 days compressive strength (MPa)	Concrete grade
B1	4%-0.45	300	0.60	772	1158	2426	120/175	40	15.3	27.1	C20/25
B2	4%-0.45	360	0.70	671	1007	2410	145/200	225	11.1	21.5	C16/20
B3	4%-0.45	400	0.60	669	1004	2390	165/230	215	15.3	26.4	C20/25
B4	4%-0.45	400	0.55	701	1051	2395	160/230	168	17.8	30	C25/30
B5	6%-0.45	400	0.60	669	1004	2389	130/200	215	21.2	35.8	C28/35
B6	6%-0.45	400	0.55	701	1051	2469	125/200	135	24.7	44	C32/40
B7	8%-0.45	400	0.55	701	1051	2464	90/150	225	38.4	53.6	C40/50
B8	4%-1	400	0.55	701	1051	2519	80/135	160	25.8	47.8	C35/45
B9	6%-1	400	0.55	701	1051	2447.5	60/110	203	33.9	62.7	C49/60
B10	8%-1	400	0.55	701	1051	2420	40/70	240	33.7	64.4	C49/69

Note: The setting time of the AASCs in satge B are reported in the above Table based on observations during casting concrete.

Table 5: Total Cl^-, free Cl^-, and bound Cl^- values for stage B mixes

Mix No.	Mix details (Na_2O%-Ms)	Binder (kg/m^3)	w/b	Total Cl^- (Quantity)	Free Cl^- (Quantity)	Bound Cl^- (Quantity)
B1	4%-0.45	300	0.60	7.08	2.93	4.15
B2	4%-0.45	360	0.70	7.14	2.59	4.55
B3	4%-0.45	400	0.60	10.32	4.02	6.30
B4	4%-0.45	400	0.55	13.53	3.54	9.99
B5	6%-0.45	400	0.6	12.71	4.54	8.17
B6	6%-0.45	400	0.55	10.69	4.01	6.68
B7	8%-0.45	400	0.55	7.72	3.14	4.58
B8	4%-1	400	0.55	11.37	4.62	6.75
B9	6%-1	400	0.55	11.36	3.69	7.67
B10	8%-1	400	0.55	9.32	3.53	5.79

Note: Quantity of total Cl^- and free Cl^- was estimated by computing the area under the concentration vs depth curve. Maximum value for depth was 16mm for all mixes. Quantity of bound chlorides is therefore the difference between the total and free chlorides.

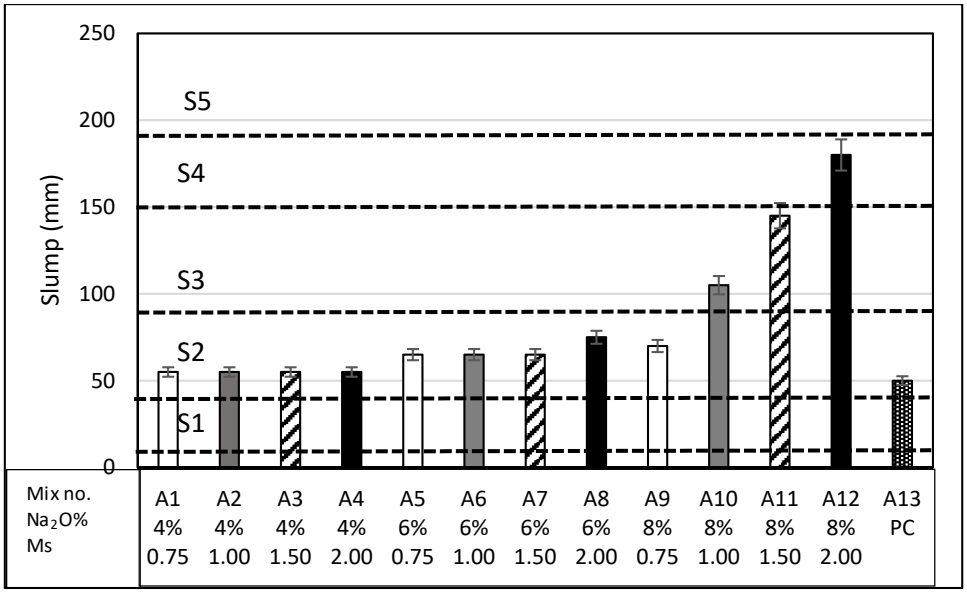

337

338 (a)

339

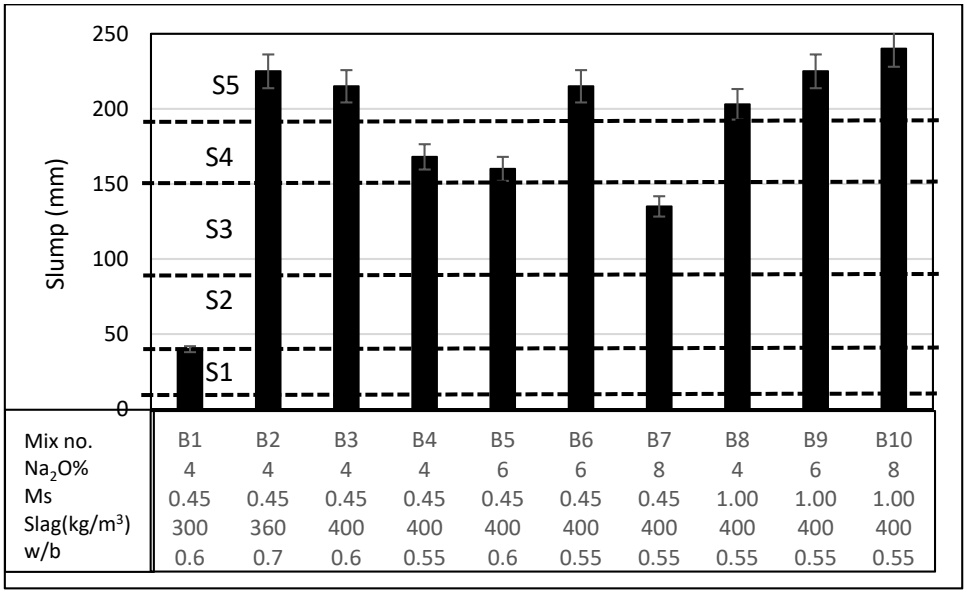

340

341 (b)

342 Figure 1. Slump results of AAS concretes: (a) Stage A, water to binder ratio = 0.47 and binder content
343 = 400 kg/m^3; (b) Stage B with various mix design parameters as marked

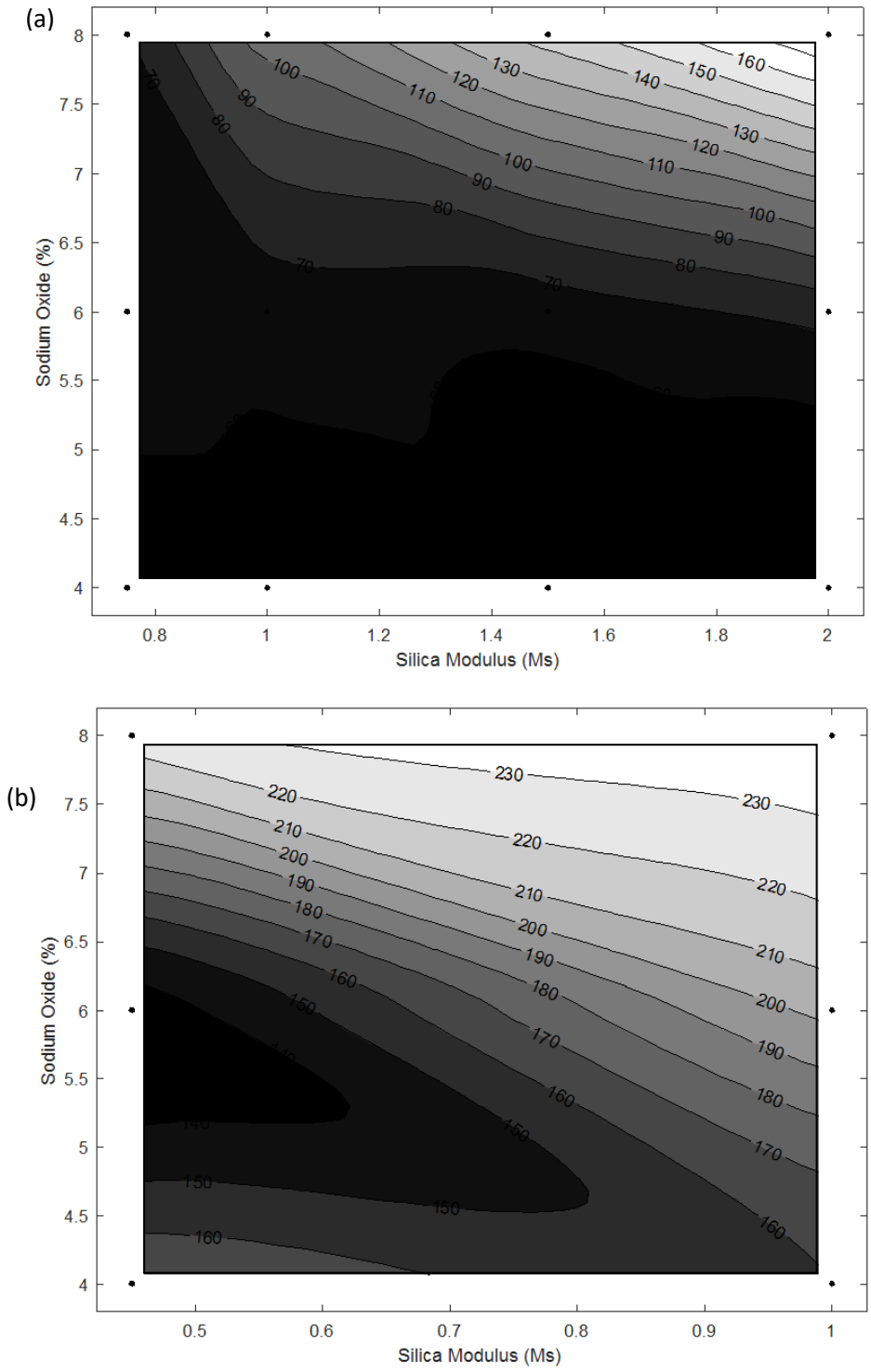

Figure 2. Contour graph for workability of different mixes (binder content=400 kg/m^3): (a) Stage A, water to binder ratio = 0.47; (b) Stage B, water to binder ratio = 0.55

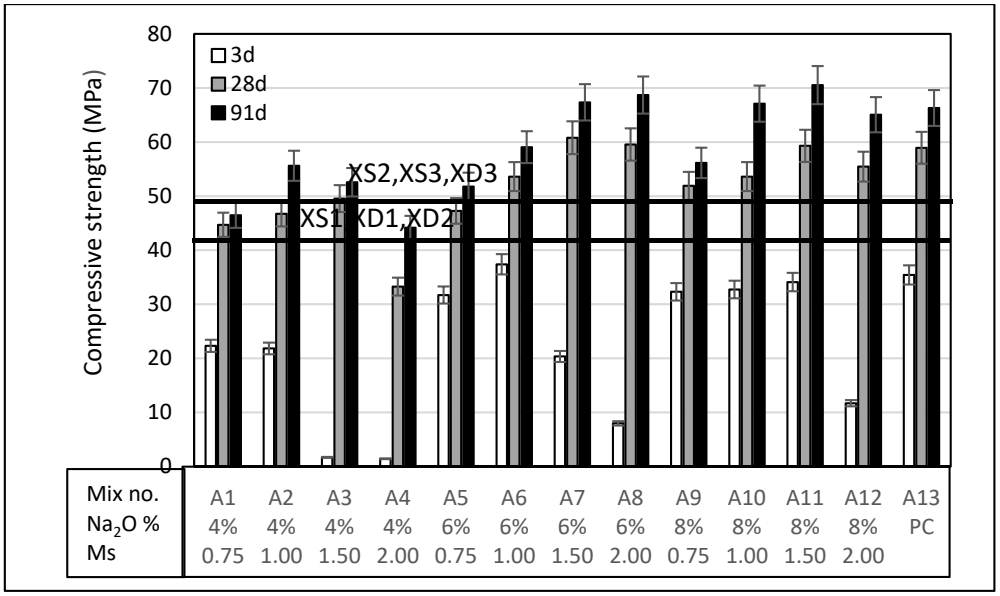

(a)

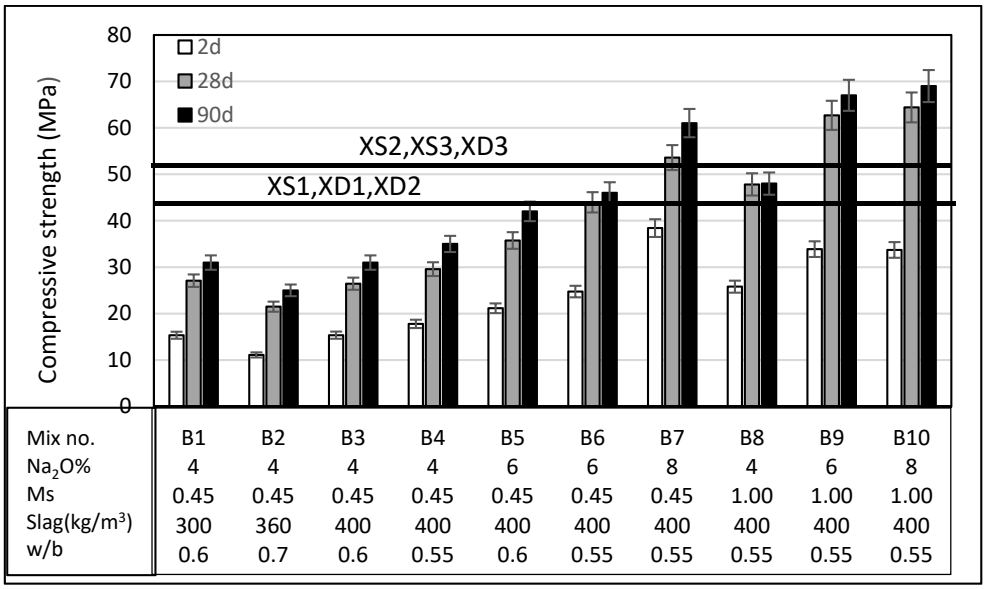

(b)

Figure 3. Strength results of AAS concretes at different curing ages: (a) Stage A, water to binder ratio = 0.47 and binder content = 400 kg/m^3; (b) Stage B with various mix design parameters as marked. The error bar compare the difference between the mean with the amount of scatter within replicates.

(a)

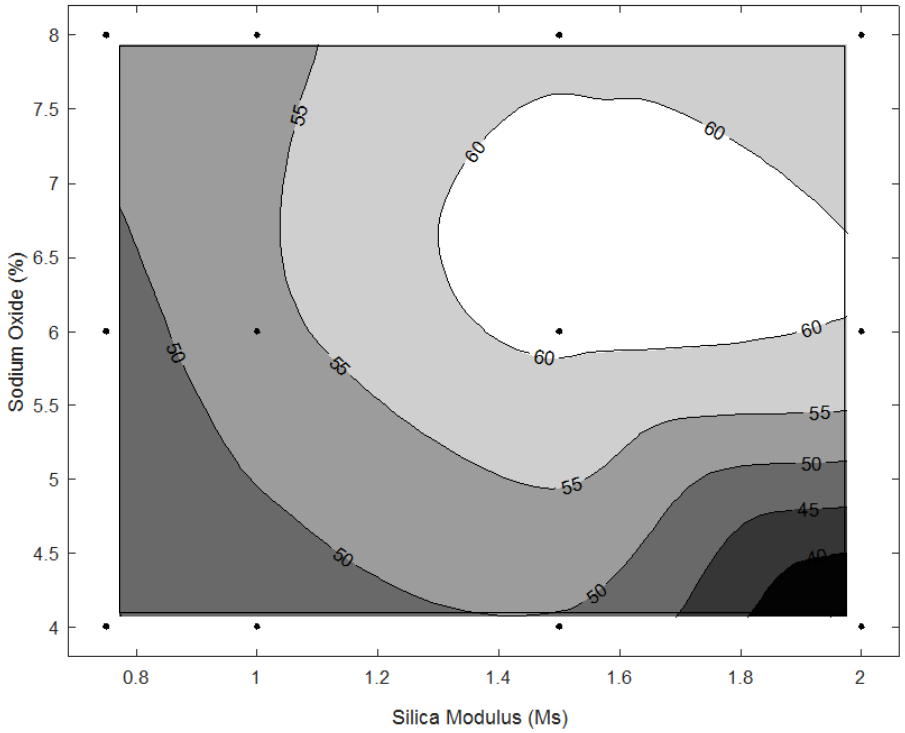

(b)

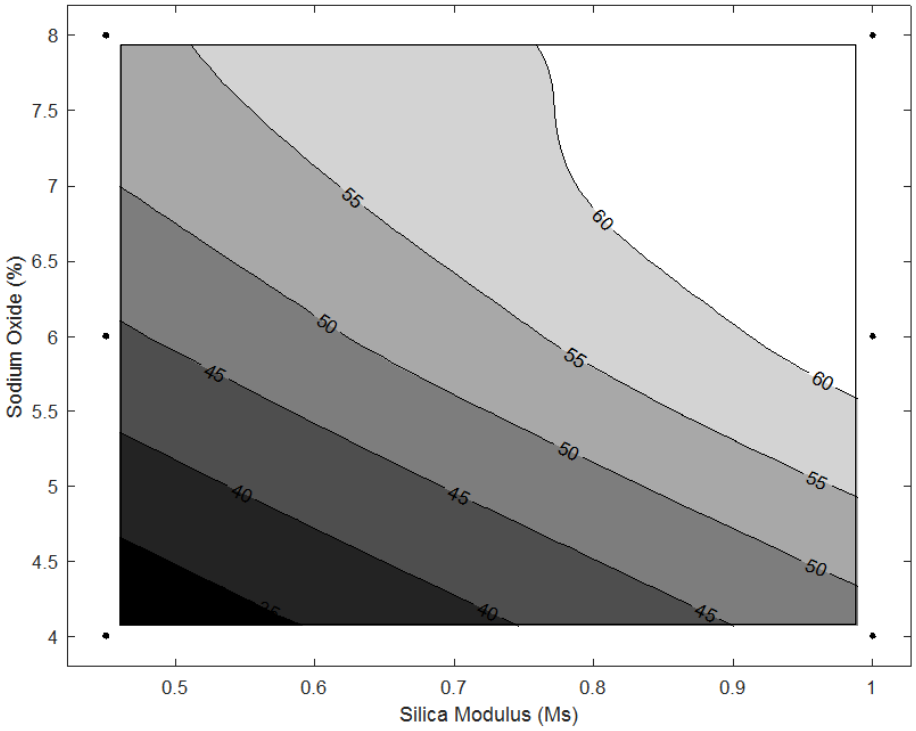

Figure 4. Contour graph for 28 days compressive strength of different mixes (binder content = 400 kg/m^3): (a) Stage A, water to binder ratio = 0.47; (b) Stage B, water to binder ratio = 0.55.

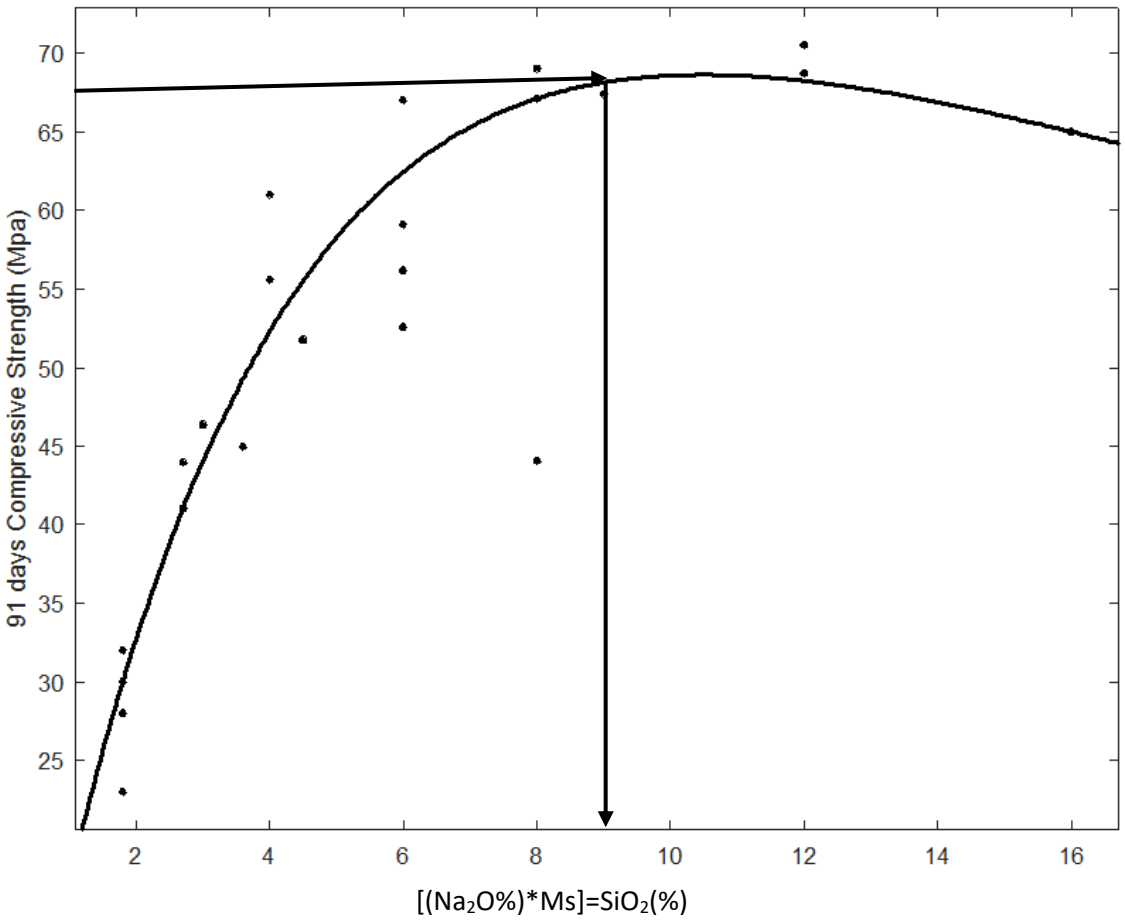

368

369 Figure 5. Correlation of 91 days compressive strength and SiO_2 content in activator of AAS concrete

Fit found when optimization terminated:

General model Exp2:
f(x) = a*exp(b*x) + c*exp(d*x)
Coefficients (with 95% confidence bounds):
a = 92.67 (16.16, 169.2)
b = -0.02089 (-0.07184, 0.03005)
c = -95.84 (-155.7, -35.99)
d = -0.2671 (-0.539, 0.004749)

Goodness of fit:
SSE: 312.5
R-square: 0.9315
Adjusted R-square: 0.9201
RMSE: 4.166

370

371

372

373

374

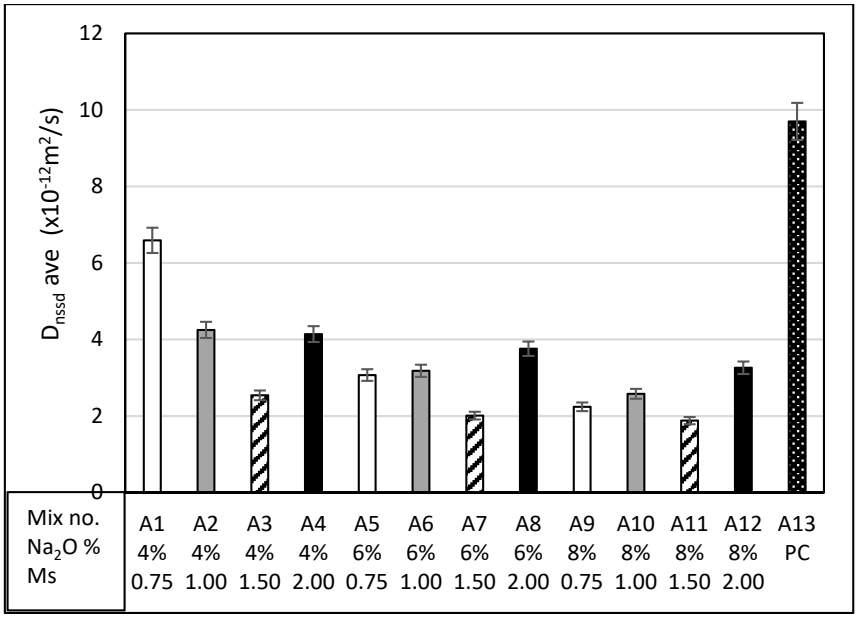

(a)

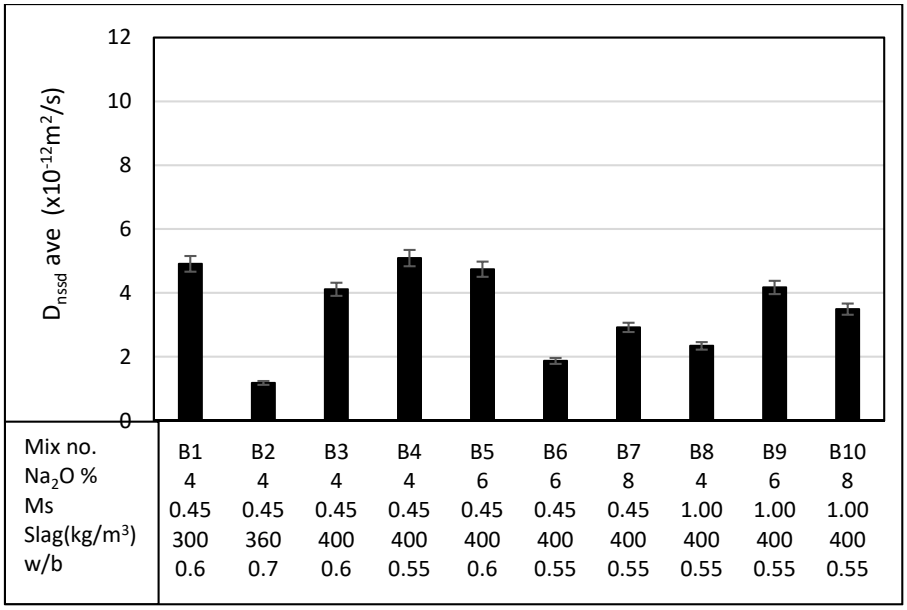

(b)

Figure 6 D_{nssd} values measured for AAS concrete mixes: (a) Stage A- water to binder ratio=0.47 and binder content = 400 kg/m^3 (b) Stage B

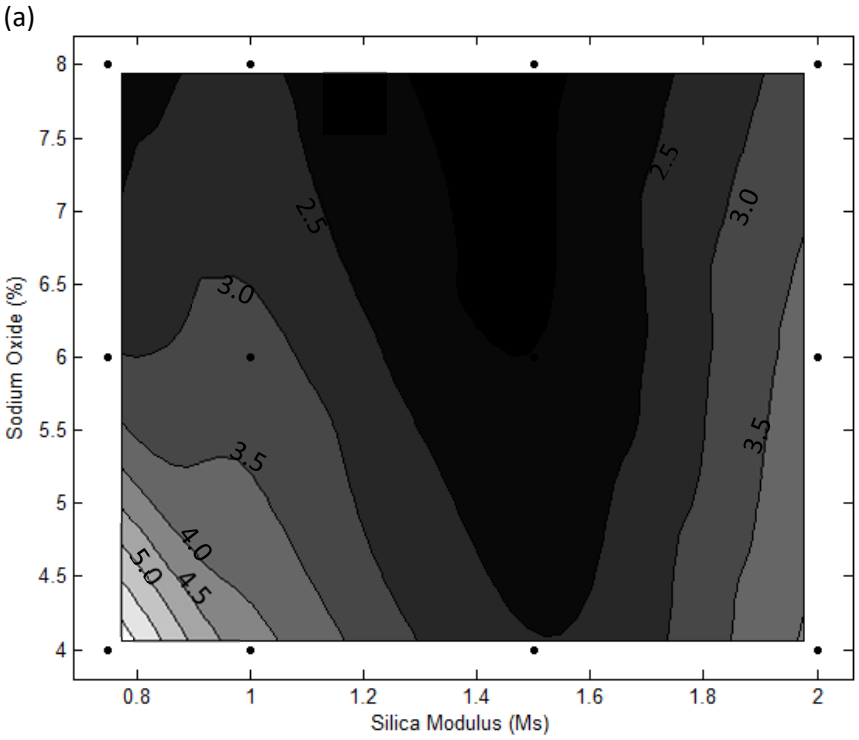

381

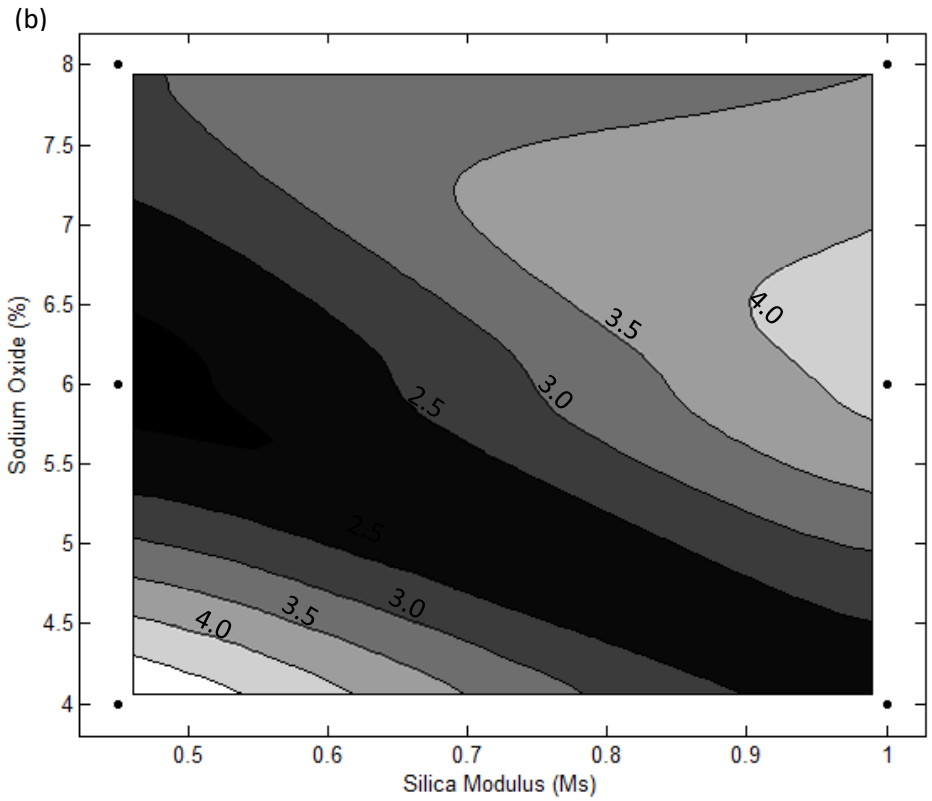

382

383 Figure 7 Contour graphs for D_{nssd} ($\times 10^{-12}$ m^2/s) of different mixes (binder content = 400 kg/m^3): (a)

384 Stage A, water to binder ratio = 0.47; (b) Stage B, water to binder ratio = 0.55

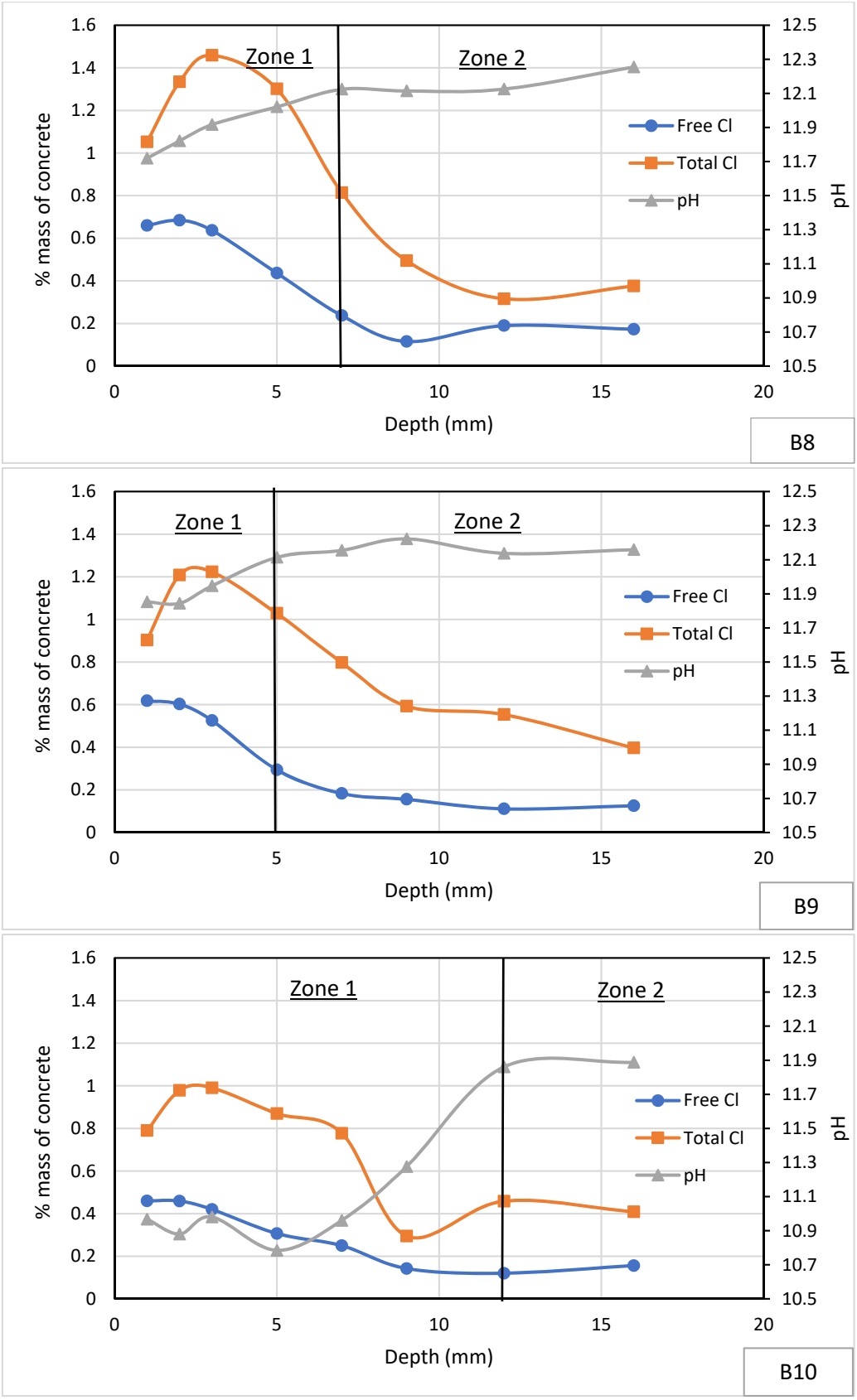

Figure 8 Total and water-soluble Cl^- and pH of mixes B8, B9 and B10 of stage B

Acknowledgements

This work was supported by the United Kingdom Engineering and Physical Sciences Research Council (EPSRC) under grant EP/M003272/1, awarded jointly with NSFC (China). The authors gratefully acknowledge Dr. Y. Bai and Professor C. Yang for their technical guidance in data generated in stage A of this work.

References

[1] Whiting, J., (1895), "Manufacture of Cement", U.S. Patent 544,706

[2] Provis, J.L., van Deventer, J.S.J. eds., (2014), Alkali Activated Materials, State-of-the-Art Report, RILEM TC 224-AAM. RILEM/Springer: Dordrecht.

[3] Wang, S.D., Scrivener, K.L., Pratt, P.L., (1994), "Factors affecting the strength of alkali-activated slag", Cement and Concrete Research, 24(6), 1033-1043

[4] Shi, C., Krivenko, D., Roy, P., (2006), Alkali Activated Cements and Concretes, Taylor & Francis:London.

[5] Krizan, D., Zivanovic, B., (2002), "Effects of dosage and modulus of water glass on early hydration of alkali-slag cements", Cement and Concrete Research, 32 (8), 1181-1188

[6] Fernández-Jiménez, A., Puertas, F., (2003), "Effect of activator mix on the hydration and strength behavior of alkali-activated slag cements", Advances in Cement Research, 15(3), 129-136

[7] Bernal, S.A., Mejía de Gutiérrez, R., Pedraza, A.L., Provis, J.L., Rodríguez, E.D., Delvasto, S., (2011), "Effect of binder on the performance of alkali-activated slag concretes", Cement and Concrete Research, 41(1), 1-8

[8] Park, J.W., Ann, K.Y., Cho, C.G.(2015), "Resistance of alkali-activated slag concrete to chloride-induced corrosion", Advances in Materials Science and Engineering, Article ID 273101, 7 pages

[9] Ma, Q., Nanukuttan, S.V., Basheer, P.A.M., Bai, Y., Yang, C. (2016) "Chloride transport and the resulting corrosion of steel bars in alkali activated slag concretes", Materials and Structures, 49(9), 363-3677

[10] BS EN 206 (2013) Concrete —Part 1: Specification, performance, production and conformity, BSI, London

[11] BS 1881-125 (2013) Testing Concrete-Part 125: Methods for mixing and sampling fresh concrete in the laboratory, BSI, London

[12] BS EN 12350-2 (2009) Testing fresh concrete - Part 2: Slump test, BSI, London

[13] BS EN 12390-3 (2009) Testing hardened concrete - Part 3: Compressive strength of test specimens, BSI, London

[14] NT BUILD 443 (1995) Concrete, hardened: accelerated chloride penetration, NORDTEST, Espoo.

[15] RILEM TC 178-TMC: "Testing and modelling chloride penetration in concrete. Analysis of total chloride content in concrete, recommendation", Materials and Structures (2002), 35, 583-585

[16] RILEM TC 178-TMC: "Testing and modelling chloride penetration in concrete. Analysis of water soluble chloride content in concrete, recommendation", Materials and Structures (2002), 35, 586-588

[17] Collins, F.G., Sanjayan, J.G., (1999) "Workability and mechanical properties of alkali activated slag concrete", Cement and Concrete Research, 29(3), 455-458

[18] BS 8500-1 (2015) Concrete—complementary British Standard to BS EN 206-1—part 1: method of specifying and guidance for the specifier, BSI, London

[19] Allahverdi, A., Shaverdi, B., Najafi Kani, E., (2010) "Influence of sodium oxide on properties of fresh and hardened paste of alkali-activated blast-furnace slag", International Journal of Civil Engineering, 8(4), 304-314

[20] Yang, T.R., Chang, T.P., Chen, B.T., Shih, J.Y., Lin, W.L. (2012) "Effect of alkaline solutions on engineering properties of alkali-activated GGBFS paste", Journal of Marine Science and Technology, 20(3), 311-318

[21] Krizan, D., Zivanovic, B., (2002), "Effect of dosage and modulus of water glass on early hydration of alkali slag cement", Cement and Concrete Research, 32(8), 1181-1188

[22] Winnefeld, F., Ben Haha, M., Le Saout, G., Costoya, M., Ko, S.-C., Lothenbach, B. (2015) "Influence of slag composition on the hydration of alkali-activated slags", Journal of Sustainable Cement-Based Materials, 4(2), 85-100.

[23] Ravikumar, D., Neithalath, N., (2012), "Effects of activator characteristics on the reaction product formation in slag binders activated using alkali silicate powder and NaOH", Cement and Concrete Composites 34(7), 809-818

[24] Lloyd, R.R., Provis, J.L., van Deventer, J.S.J., (2010), "Pore solution composition and alkali diffusion in inorganic polymer cement", Cement and Concrete Research, 40(9), 1386-1392

[25] Beushausen, H., Fernandez Luco, L. eds, (2016) Performance-Based Specifications and Control of Concrete Durability, State-of-the-Art Report, RILEM TC 230-PSC, RILEM/Springer: Dordrecht.

[26] PD CEN/TR 16563 (2013) Principles of the equivalent durability procedure, CEN, Brussels.

[27] van Deventer, J.S.J., San Nicolas, R., Ismail, I., Bernal, S. A., Brice, D. G., Provis, J. L., (2014) "Microstructure and durability of alkali-activated materials as key parameters for standardization", Journal of Sustainable Cement-Based Materials, 4(2), 116-128

[28] Ravikumar, D., Neithalath, N., (2013), "Electrically induced chloride ion transport in alkali activated slag concretes and the influence of microstructure", Cement and Concrete Research 47, 31-42

[29] Ismail, I., Bernal, S. A., Provis, J. L., San Nicolas, R., Brice, D. G., Kilcullen, A. R., Hamdan, S., van Deventer, J. S.J., (2013) "Influence of fly ash on the water and chloride permeability of alkali-activated slag mortars and concretes", Construction and Building Materials, 48, 1187–1201

[30] Ke, X., Bernal, S. A., Provis, J. L., (2017) "Uptake of chloride and carbonate by Mg-Al and Ca-Al layered double hydroxides in simulated pore solutions of alkali-activated slag cement", Cement and Concrete Research 100, 1–13

[31] Ke, X., Bernal, S. A., Hussein, O. H., Provis, J. L., (2017) "Chloride binding and mobility in sodium carbonate-activated slag pastes and mortars", Materials and Structures, 50: #252

[32] Backus, J., McPolin, D., Basheer, M., Long, A., Holmes, N. (2013), "Exposure of mortars to cyclic chloride ingress and carbonation", Advances in Cement Research, 25(1), 3-11

[33] Castellote, M., Andrade, C., Alonso, C., (1999) "Chloride-binding isotherms in concrete submitted to non-steady-state migration experiments", Cement and Concrete Research, 29, 1799-1806

[34] Tang, L., Nilsson, L., (1993) "Chloride binding capacity and binding isotherms of OPC pastes and mortars, Cement and Concrete Research, 23(2), 247– 253

[35] Luo, R., Cai, Y., Wang, C., Huang, X., (2003) "Study of chloride binding and diffusion in GGBS concrete", Cement and Concrete Research, 33(1), 1 –7

[36] BS EN 197-1 (2011) Cement. Composition, specifications and conformity criteria for common cements (incorporating corrigenda November 2011 and October 2015), BSI, London

[37] Ma, Q. (2013), Chloride transport and chloride induced corrosion of steel reinforcement in sodium silicate solution activated slag concrete, PhD Thesis, Queens University of Belfast, Northern Ireland, UK.